AEDC-TR-68-235

cy. 6

NONINTERFERENCE VELOCITY MEASUREMENTS IN A SUPERSONIC SEEDED PLASMA USING TRACERS PRODUCED BY A SPARK DISCHARGE AND A FOCUSED PULSED LASER

J. C. Pigott and L. E. Rittenhouse

ARO, Inc.

November 1968

PROPULSION WIND TUNNEL FACILITY
ARNOLD ENGINEERING DEVELOPMENT CENTER
AIR FORCE SYSTEMS COMMAND
ARNOLD AIR FORCE STATION, TENNESSEE

NOTICES

When U. S. Government drawings specifications, or other data are used for any purpose other than a definitely related Government procurement operation, the Government thereby incurs no responsibility nor any obligation whatsoever, and the fact that the Government may have formulated, furnished, or in any way supplied the said drawings, specifications, or other data, is not to be regarded by implication or otherwise, or in any manner licensing the holder or any other person or corporation, or conveying any rights or permission to manufacture, use, or sell any patented invention that may in any way be related thereto.

Qualified users may obtain copies of this report from the Defense Documentation Center.

References to named commercial products in this report are not to be considered in any sense as an endorsement of the product by the United States Air Force or the Government.

NONINTERFERENCE VELOCITY MEASUREMENTS IN A SUPERSONIC SEEDED PLASMA USING TRACERS PRODUCED BY A SPARK DISCHARGE AND A FOCUSED PULSED LASER

J. C. Pigott and L. E. Rittenhouse
ARO, Inc.

FOREWORD

The work presented herein was sponsored by Headquarters, Arnold Engineering Development Center (AEDC), Air Force Systems Command (AFSC), under Program Element 6540215F, Project 4344, Task 434409.

The work was done and the results prepared by ARO, Inc. (a subsidiary of Sverdrup & Parcel and Associates, Inc.), contract operator of AEDC, AFSC, Arnold Air Force Station, Tennessee, under Contract F40600-69-C-0001. The work was conducted from November 1966 to July 1968 under ARO Project No. PL3751 and PL3851, and the manuscript was presented for publication on September 24, 1968.

The authors wish to thank W. Beyermann of the Marquardt Corporation and Dr. J. Trollinger of ARO, Inc., for consulting services regarding the laser used during the tests.

This technical report has been reviewed and is approved.

Burnell B. Algee
Captain, CAF
Research Division
Directorate of Plans
and Technology

Edward R. Feicht
Colonel, USAF
Director of Plans
and Technology

ABSTRACT

Experimental results are presented from a program conducted to develop a noninterference method for obtaining the velocity of a supersonic, high enthalpy plasma seeded with an alkali metal. The technique used was the time-of-flight measurement of a tracer spark produced in the plasma by an electric spark discharge (two pointed electrodes) and by a focused pulse laser. The tracer spark was photographed with a streak and framing camera or an image-converter camera at preselected delay times to obtain the time-of-flight velocity measurements. The experimental work was accomplished in air and nitrogen plasmas, at a static pressure of about 1 atm and at total enthalpies up to 2700 Btu/lb. Velocities were measured up to 2600 m/sec. The techniques used are described, and the problems and results are discussed.

CONTENTS

APPENDIX
Illustrations

SECTION I
INTRODUCTION

Pitot-static and total enthalpy probes have been used for many years to measure the gas dynamic properties of supersonic gases from which the gas velocity can be calculated. However, with the current trend toward high enthalpy flows, the use of the aforementioned probes has become rather limited. In the first place the heat loads imposed on the probes from the high enthalpy gas have become very high, thus requiring complicated water-cooled design or precluding measurement because of probe material considerations. Secondly, the transport properties of the high enthalpy gas are not always known, particularly behind the bow shock wave; thus, the use of gas dynamic equations involving the measured gas properties is suspect. Furthermore, the addition of alkali compounds to the flowing gas in order to increase the electrical conductivity for magnetohydrodynamic (MHD) application further complicates the preceding problems. Therefore, it is evident that a direct velocity measurement obtained by a noninterference technique, wherein a probe is not immersed in the flowing gas, is very desirable.

Several noninterference velocity measurement techniques are reported in the current literature. The technique which appears to be most applicable to high velocity, high enthalpy flows is to determine the time-of-flight of a tracer spark introduced into the flowing gas. Several investigators have reported work in this direction. Kyser (Ref. 1) has successfully measured the velocity in hypervelocity flow fields by photographing the displacement with time of multiple sparks. Miller (Ref. 2) has measured the velocity in the hot-shot-type tunnels by photographing the displacement of both a spark and the blast wave from the spark. Woods and Carter (Ref. 3) have measured the velocity in a cesium-seeded plasma at the exit of an MHD accelerator using the spark displacement technique. Chen (Ref. 4) has photographed and measured velocity profiles from the luminous spot produced by a focused pulse laser. Similar work has been done with the laser luminosity using photomultiplier cells to observe the luminosity (Ref. 5).

The purpose of the investigation reported herein was to develop a noninterference technique for measuring the velocity of a high enthalpy, supersonic, seeded plasma. The technique investigated was the optical tracing of a tracer spark produced by an electrical discharge from pointed electrodes and by a focused pulse laser. This technique had been investigated previously by the above-referenced authors; however, the

flow conditions were sufficiently different from those previously investigated to require additional testing and development of the technique.

The tests were conducted at the exit of a nominally rated 2-Mw electric arc heater which discharged as a free jet to the atmosphere. The test facility used was not particularly suited for this investigation since the flow was not steady, and the velocity at the exit of the arc heater was not known exactly. Moreover, it is known that the gas velocity varies as a function of the distance downstream from the nozzle exit for a free jet. However, the primary objective of this investigation was to develop a technique for measuring the velocity in seeded and unseeded plasmas and not to analyze the flow from this particular arc heater. It would have been advantageous for these tests if a steady flow of known velocity could have been used. However, an arc-heated facility, which inherently is a nonsteady flow device, is necessary in order to produce the high enthalpy flows of interest in this investigation.

SECTION II
GENERAL TEST EQUIPMENT

The basic components of the experimental apparatus were the electric arc heater, electrode spark system, laser spark system, cameras, seeding system, and magnet. These components are discussed in this section.

2.1 ELECTRIC ARC HEATER

A gas-stabilized arc heater operating from a d-c power supply was used to heat nitrogen or air and thus produce the plasma test media (see Fig. 1, Appendix). The gas flow was parallel to the arc column in the arc heater and issued into a stilling chamber before entering a supersonic nozzle. The gas was then expelled through the supersonic nozzle to the atmosphere as a free jet. The arc heater, stilling chamber, and supersonic nozzle sections were cooled with demineralized, high pressure water. The arc heater power input, mass flow rate, and water coolant losses were monitored so that an energy balance could be made. The arc heater was operated with a power input of approximately 1.2 Mw at a mass flow rate from 0.20 to 0.22 lb/sec of either air or nitrogen. The electrical-to-thermal conversion efficiency of the arc heater, including stilling chamber and supersonic nozzle losses, was approximately 50 percent.

The typical range of flow conditions at the exit of the 2.54- by 2.54-cm-square supersonic nozzle was:

Total pressure, 2.8 to 3.5 atm
Total enthalpy, 700 to 2700 Btu/lb
Mach number, approximately 1.7
Seeding rate (potassium or cesium), 0.3 mole percent

Some of the experimental data were obtained with an extension to the supersonic nozzle which should have produced an exit Mach number greater than 1.7. However, after the tests were completed, it was obvious that the pressure ratio across the nozzle, plus extension, was not sufficient to maintain fully supersonic flow. The velocity measurements taken downstream of the nozzle extension indicated the flow velocity was varying with time and at near-sonic Mach numbers most of the time. This situation would be expected if the supersonic nozzle was not filled.

2.2 SEEDING SYSTEM

Potassium carbonate (K_2CO_3) and cesium carbonate (Cs_2CO_3) in powder form were used as seeding materials. The seed material was dispensed by a commercial powder feeder and injected into the arc heater with a nitrogen carrier gas at the point shown in Fig. 1. The seeding unit was calibrated before and after each run to ensure that the desired seed flow rate was obtained.

2.3 ELECTRODE SPARK SYSTEM

The electric spark tracer used in a portion of the experimental investigation was produced by discharging the stored energy from a capacitor between the tips of the two tungsten electrodes. The electrodes were positioned downstream of the nozzle, at the edge of the plasma flow, where the spark would discharge across the plasma.

Initially, a 0.06-μf capacitor was used, charged to 15 kv (stored energy of 6.75 joules). The discharge was controlled by a hydrogen-filled thyratron (Fig. 2). Experiments with this power source showed that a faster, high current discharge was needed. A new power source was constructed, using a coaxial arrangement of parts in order to hold the circuit inductance to the smallest possible value (Fig. 3). Energy was stored in a 0.1-μf capacitor charged to 50 kv (125 joules), and the discharge was controlled by a triggered gas-filled spark gap.

The discharge current which this power source produced could not be measured directly. However, the derivative of the current was obtained by placing a small, thoroughly shielded pickup loop near the output lines to the spark gap. The loop was connected to an oscilloscope by a length of coaxial cable, which was terminated in its characteristic impedance to eliminate reflections. The wave-form was recorded by photographing the oscilloscope display. The power source, leads, and spark gap were assumed to form a series RLC circuit, the value of C (capacitance) being known. The resistance and inductance were determined from the current derivative wave-form by measuring the time to the first zero crossing and the ratio of the height of the first and second peaks. These measurements indicated a peak current of 11,000 amp, a damping factor of about 0.6, and a time to the first current zero of about 0.75 μsec. Nearly the entire stored energy is dissipated by the time of the first current zero.

2.4 LASER SPARK SYSTEM

A standard Korad K-1Q pulsed ruby laser system was used with the necessary optics to produce an intense optical frequency electric field at a focal point in the plasma, thus producing a luminous laser spark (see Fig. 4). The components of the laser system included a K-1Q Pockell's cell Q-switch, the laser head with a 9/16- by 4-in. standard quality ruby rod, a front reflector, a K-1Q power supply and electronics, and a refrigerated water cooler. The rated capability of the laser system was 125 to 150 Mw.

The Pockell's cell and laser head were carefully aligned according to the Korad instruction manual. The optical system was aligned with the aid of a continuous wave laser.

The lenses were inserted along the laser axis, so that the left focal point of Lenses L_1 and L_2 coincided (see Fig. 5). A beam of parallel light was produced between Lenses L_2 and L_3. Lens L_3 focused the laser energy to a point in the plasma where breakdown of the gas occurred. The spark could be moved horizontally across the plasma by moving Lens L_3 on the optical bench. The size and type of lenses used are shown in Fig. 5. Since the laser light is monochromatic, lenses corrected for chromatic aberrations are not necessary; however, spherical aberrations are still important, and the lenses were corrected to obtain a definite focal point.

2.5 CAMERAS

A Beckman and Whitley Model 200, 12-frame, simultaneous streak and framing camera and a Beckman and Whitley image-converter camera were used to photograph the displacement of the tracer spark in the plasma. Both cameras will be discussed in this section.

2.5.1 Simultaneous Streak and Framing Camera

The simultaneous streak and framing camera used was a rotating mirror camera which could simultaneously record 12 frames of an event on a film plate and at the same time, produce a streak record of the event. A schematic of the camera is shown in Fig. 6, and the test installation is shown in Fig. 7. The camera was capable of recording up to 4,000,000 pictures per second, which represents an interframe interval of 0.25 μsec. The camera was equipped with a 1/50-sec capping shutter which is opened when the rotating mirror reaches a preset speed and is closed at a predetermined time thereafter. Since the capping shutter is very slow relative to the rotating mirror speed, camera rewrite of the event background is a problem if the background luminosity is very intense. This problem occurred when the plasma was seeded. Camera rewrite of the seeded plasma overexposed the film and precluded the use of this camera for most of this experimental investigation.

2.5.2 Image-Converter Camera

The camera requirements for this work were large size, distortion-free, nanosecond exposures of the spark event with a minimum light loss. An image-converter camera, which is a high-speed, electronic device, was an obvious choice to meet these requirements. A schematic of the image-converter camera is shown in Fig. 8, and the test installation is presented in Fig. 9. An image of the object is focused on the planar photocathode of the camera image-converter tube. When a high voltage pulse is applied to the tube between the cathode and anode, electrons with a density distribution corresponding to the light distribution of the image are accelerated from the cathode to the anode. The electrons excite the anode phosphor, recreating the image. The image is focused on the film plane by the relay optics, and the exposure time is determined by the pulse width applied to the image tube. The image-converter camera used in this investigation was capable of taking three photographs of the event. Each picture requires a separate camera head containing the image-converter tube and relay optics; however, the camera heads can be arranged in different configurations. For example,

the camera heads can be mounted separately to take pictures from different angles and locations, two camera heads can be coupled to a beam splitter if desired, or a single camera head can be mounted to a special unit which will pulse the camera at predetermined exposure and delay times to produce a triple exposure of an event on a single film plate. The last-mentioned feature was designed by Beckman and Whitley especially for this experimental program. The triple-exposure camera configuration (shown in Fig. 9) was used almost exclusively in the experimental work and greatly facilitated the reading and enhanced the accuracy of the experimental data since all the spark displacement data appeared on one piece of film. With each of the camera configurations, the operator can set the delay and exposure time for each picture frame. Exposure times of 5, 10, 50, 100, and 1000 nsec are available with delay times after the initial pulse (time equal zero) continuously variable from 0.20 to 300 μsec. The maximum image size on the film is 3.5 in. in diameter.

2.5.3 Synchronization of the Tracer Spark and the Image-Converter Camera

The tracer sparks were synchronized with the image-converter camera in the following manner. The electrical spark discharge was initiated by an external trigger to the electrode power supply. A pickup loop located near the spark electrodes received a trigger pulse from the induced electric field created by the spark discharge which was sent directly to the camera time delay and pulse generators. The delay generators triggered the cameras at the preset delay times. The initial trigger pulse from the loop and the pulses from the delay generators which triggered the image-converter camera on an oscilloscope screen and the screen were photographed. A typical oscilloscope record is shown in Fig. 10. The method of synchronizing the laser spark and the camera was identical to that just discussed, with the exception that the external pickup loop was not necessary since the laser provided an output pulse to trigger the camera delay generators.

2.6 MAGNET

A magnetic field was used in some of the experimental work to aid in collimating the electric spark discharge. It was produced parallel to the spark discharge with a water-cooled, iron-core electromagnet. The magnetic field at the electrodes could be varied from 1 to 10 kilogauss by varying the magnet current.

SECTION III
VELOCITY MEASUREMENT TECHNIQUES

3.1 ELECTRODE SPARK DISCHARGE

3.1.1 Streak and Framing Camera with 15-kv Electrode Power Supply

A typical photograph of the spark discharge between pointed electrodes in an unseeded nitrogen plasma using the streak and framing camera is shown in Fig. 11a. For these tests the plasma total enthalpy was 2400 Btu/lb, and the total pressure was 2.8 atm. The Mach number at the exit of the nozzle was approximately 1.7. The numbers to the left of the framing photograph indicate the time sequence in which the exposures were made. The luminosity of the tracer spark persisted at least 16 μsec for both nitrogen and air plasmas. The streak photographs could be used for velocity measurements; however, the quality of the photographs was not sufficient for reproduction in the report. The photographs presented in Fig. 11 were obtained with the electrodes placed 2.54 cm downstream from the nozzle exit and 3.2 cm apart.

Another example of the excellent flow visualization made possible by the electric spark discharge is shown in Fig. 11b. Conditions were identical for Figs. 11a and b. However, in Fig. 11b the lower electrode was protruding slightly into the plasma. The resulting flow perturbations are shown by the displacement of the spark. A photograph of the spark in a seeded plasma is shown in Fig. 11c. The test conditions for this photograph are identical to those in the previous examples, except the plasma has been seeded with 0.3-mole percent potassium. Potassium carbonate was the seed material used. It can be noted that the light intensity of the plasma has been greatly increased as compared to the preceding photographs and that the light radiated from the plasma has completely washed out the photograph. It is impossible to discern the arc column, if it exists, in the plasma.

As described previously, the Beckman and Whitley Model 200 camera is a rotating mirror camera with a 1/50-sec capping shutter. Because the shutter speed is very slow relative to the camera framing speed, the camera makes many exposures of the background while the capping shutter is open. Since the light intensity of the seeded plasma is many times greater than that of the unseeded plasma, the camera rewrite overexposed the film plate to the degree that the spark could not be seen in the plasma.

In an attempt to circumvent this problem, a Kerr cell was inserted in front of the camera lens to act as a high-speed capping shutter and thus prevent camera rewrite. The Kerr cell was an effective shutter, but, because it is a relatively high light loss device, the light transmitted by the Kerr cell was very marginal for the camera exposure times available. In fact, the photographs were underexposed, and a velocity determination was not possible.

At higher plasma velocities to which this technique can be applied, faster framing rates than those used are necessary, which results in shorter exposure times than those tested. Since light transmission was already very marginal with this camera-Kerr cell combination, a fast shutter speed, high efficiency, light-amplifying camera was required. The image-converter camera fulfills these requirements.

3.1.2 Image-Converter Camera with 50-kv Electrode Spark Source

The image-converter camera described earlier was used in conjunction with the 50-kv electrode spark system. The test installation, which included the nozzle extension on the arc heater, is shown in Fig. 9.

Excellent photographs of the spark were obtained in both air and nitrogen plasmas using this test configuration when the plasma was unseeded. The plasma total enthalpy was 2600 Btu/lb, and the total pressure was 3.5 atm. Typical photographs of the spark in the unseeded nitrogen plasma are shown in Fig. 12. Equally definite photographs were obtained in an air plasma. The camera delay times after the initial spark and the camera exposure times are shown for each figure. During the initial phases of testing, some difficulty was encountered with the camera so that only two exposures of the spark could be taken rather than the three for which the camera was designed. This problem was corrected, and triple-exposure photographs were obtained. The plasma conditions were maintained as nearly constant as possible during this series of data points in which the nozzle extension was used. However, as shown in Fig. 12, the profile across the plasma is not the same for all the photographs. It will be shown later that the flow was not filling the nozzle extension, resulting in near-sonic exit Mach numbers in some cases.

Typical photographs of the electric spark in the plasma without the nozzle extension on the arc heater are shown in Fig. 13. For these photographs the test conditions are the same as indicated above. The

photographs illustrate the effect of camera exposure time on the recorded spark detail. The velocity profiles obtained with this configuration are different than those shown in Fig. 12, as was the measured velocity. The flatness of the profile and the increase in measured velocity, as compared to the data with the nozzle extension, indicated that the nozzle was operating correctly.

When the plasma was seeded with either K_2CO_3 or Cs_2CO_3, the electrical conductivity and luminosity of the plasma were greatly increased. Typical photographs of the spark discharge in the seeded plasma are shown in Fig. 14. With the image-converter camera the film was not overexposed, as was the case with the framing camera, when the plasma was seeded. These photographs were typical of both air and nitrogen plasmas. It can be seen that the spark is visible near the electrodes and in the mixing region of the jet but becomes diffuse and disappears in the plasma core. At very low seeding rates, the electrical discharge was sometimes visible in the plasma. At seed rates of 0.3 mole percent, which corresponds to an electrical conductivity of approximately 400 mho per meter, sufficient charge carriers are present in the plasma to conduct the electrode current without requiring a spark process to occur. The spark was never visible in the plasma at this seeding rate, although many attempts were made. From these tests it is concluded that the discharge is not sufficiently collimated in a seeded plasma to permit the use of optical methods for a velocity measurement.

3.1.3 Image-Converter Camera with 50-kv Electrode Spark Discharge in a Parallel Magnetic Field

A parallel magnetic field was applied to the electric discharge between the electrodes in an attempt to collimate the spark and make it visible in the seeded plasma. Magnetic fields from 1 to 10 kilogauss were applied with the magnet installation shown in Fig. 15. It was found that magnetic fields up to 2 kilogauss somewhat aided in collimating the spark; however, little additional effect on the spark in the seeded plasma was noted at higher magnetic fields. The spark could be photographed fairly consistently at seeding rates to 0.15 mole percent with magnetic fields of 1 to 2 kilogauss. Without a magnetic field, the spark was not visible in the plasma at this seeding rate. The spark was not visible at higher seeding rates even when the magnetic field was increased to 10 kilogauss. Thus, it was found that the magnetic field did not significantly aid in making the spark visible in a high conductivity plasma.

3.1.4 Image-Converter Camera with Shadowgraph System

Several authors, see Ref. 2 for example, have measured the velocity of moving gases by photographing the displacement of the blast wave with time from a spark discharge. Since the spark luminosity produced by the electrodes was not visible in the seeded plasma, a shadowgraph system was set up to determine if the density gradient created by the electrical discharge or the blast wave could be made visible with a shadowgraph system. A schematic of the shadowgraph system used is shown in Fig. 16. Typical photographs of the blast wave and density gradients from the spark in quiescent air using this system are shown in Fig. 17. These photographs were taken with the delay times shown. The blast wave in a low velocity nitrogen flow (approximately 100 m/sec) is shown in Fig. 18. It can be seen that even the low velocity flow begins to perturb the blast wave and density gradients. Figure 19 is a shadowgraph photograph of the spark in an unseeded nitrogen plasma, and as is evident from the photograph, the plasma is so turbulent that little can be discerned from the photograph.

It is concluded from the work described in Section 3.1 that the electrode spark discharge technique can be used to produce tracers that can be photographed directly in an unseeded plasma from which velocity measurements can be made. However, this method of producing a tracer spark is not applicable to seeded plasmas at the test conditions of this experiment.

3.2 LASER SPARK

The use of a giant-pulse ruby laser beam focused to a discrete point to produce immense power densities has been investigated for several years. The observance of the breakdown of gases initiated by the intense optical frequency electrical field at the focal point has been investigated and reported in many references, for example, Refs. 6, 7, and 8. The use of laser sparks as tracers for making time-of-flight velocity measurements has been reported in Ref. 4 for argon and in Ref. 5 for combustion gases. In the preceding work, an electrostatic probe, a drum camera, or photomultiplier cells was used to trace the ionized spot produced by the laser. These methods of tracking the spark give little if any information regarding the geometry of the laser spark, and since the luminous spark size changes with time, the results are sometimes misleading. In this investigation, the image-converter camera was used to photograph the spark directly; thus, the spark configuration was known at the beginning and end of each time interval.

The test program using the pulse laser was initiated specifically to determine whether (1) a laser beam could be focused to produce a luminous spark in a high enthalpy, highly turbulent plasma; (2) the luminosity of the spark would be intense enough that it could be distinguished photographically from the plasma; (3) the luminosity of the spark would remain visible long enough to make time-of-flight measurements; and (4) the addition of alkali compounds would affect or prevent the creation of a laser spark by absorption and scattering of the laser light.

The installation of the laser, camera equipment, and arc heater is shown in Fig. 20. The laser was positioned so that the laser spark was initiated in the plasma approximately 1.9 cm downstream of the arc heater nozzle. The image-converter camera was located so that it viewed directly down on the laser spark by means of a mirror.

Typical photographs of the laser spark luminosity produced in the plasma are shown in Fig. 21. Figure 21a is a photograph of the laser spark in nitrogen. Figures 21b and c are photographs of the spark in nitrogen and air seeded with 0.3 mole percent of potassium.

It should be noted that the three luminous spots observed in each photograph are the same laser spark photographed with the triple-exposure image-converter camera. Because of the increased luminosity of the seeded plasma over the unseeded plasma, the seeded plasma is visible as a background in the photographs shown in Figs. 21b and c. The velocity calculation for these photographs will be presented in a later section.

An additional photograph of the laser spark is shown in Fig. 22. The laser in this photograph has been set at an angle to the flow in order to produce a spark close to the nozzle exit. One laser spark was produced in the center of the plasma as shown in the photograph. In addition, some of the laser energy passed through the focal point and ionized seed accumulations on the nozzle wall and produced a second smaller ionized spot on the edge of the plasma jet. Thus, a tracer spark was produced at the center and edge of the plasma from which velocity measurements can be made. The displacements of the two sets of sparks with time indicate a fairly constant velocity across the plasma which was expected when the nozzle extension was not used.

The threshold power required from the laser to break down the gas was not investigated during these tests; however, it was observed that the size of the spark could be changed by varying the laser power. Figure 23a

is a photograph of the laser spark in quiescent air at a medium to high power input to the laser. The size of this spark can be compared with the laser spark in air shown in Fig. 23b for a low power input to the laser. The difference in size is caused by a reduction in power to the laser and by the addition of an aperture in front of the converging lens to increase the quality of the laser beam. It also was observed during the tests that the laser spark could be created in a seeded gas stream at a laser power input too low to break down the gas without the K_2CO_3 seed addition. This can be explained by the fact that all of the K_2CO_3 particles are not ionized in the arc heater; however, they are excited. The solid particles absorb the laser energy more readily than the gas molecules, and since they may already be excited, a relatively small energy addition from the laser beam completes the ionization process, and the luminous laser spark is formed.

Thus, it is concluded that optical measurements can be made to determine the velocity of a highly turbulent plasma of high electrical conductivity using a tracer spark produced by a laser.

SECTION IV
EXPERIMENTAL AND GAS DYNAMIC CALCULATIONS OF THE PLASMA VELOCITY

4.1 EXPERIMENTAL VELOCITY DATA

The plasma velocity was calculated from the measured displacement of the tracer spark obtained from the photographs and the time between exposures from the oscilloscope pictures. Since the spark dimension was not necessarily true size on the photograph, a ruler was photographed at the electrode position to obtain the scale factor.

The tracer spark displacement could be measured in several ways, as a center-to-center, leading edge-to-leading edge, or trailing edge-to-trailing edge. As shown in the previous spark photographs, the location of the spark boundary is subject to interpretation. However, the velocity calculated using any of the above-mentioned procedures agreed reasonably well. Those photographs that were difficult to interpret or gave different spark displacements depending on the method of measurement were discarded. The displacement of the laser spark was easier to measure than the electrode spark because the boundaries of the laser spark were more definitive. As a consequence, the estimated accuracy of the laser-determined velocity is ±3 percent, whereas the velocity determined by the electrode spark is estimated to be no better than ±5 percent.

4.1.1 Streak and Framing Camera

A velocity profile across the plasma is presented in Fig. 24 and was obtained from the photographic data previously presented in Fig. 11a. The centerline velocity was calculated to be 1780 m/sec from the streak record, which compares quite favorably with the frame record. The nozzle extension on the arc heater was not used for this test, and the nozzle was operating correctly. The velocity profile shown in Fig. 24 is quite similar to impact pressure and total enthalpy profiles obtained before these tests. In general, all the velocity measurements obtained with the streak and framing camera resulted in about the same plasma velocity when operating the arc heater at about 2400 Btu/lb. However, differences in the velocity profile were obtained, and in many cases the profile was much flatter than the profile shown in Fig. 24.

4.1.2 Image-Converter Camera with 50-kv Electrode Spark Discharge

A considerable number of data points were obtained with this configuration of camera and electrode power supply. The calculated centerline velocity for the various test points is shown in Fig. 25. The nozzle extension was used with the arc heater, and as is evident in Fig. 25, the majority of the data indicate a plasma velocity of about 1400 m/sec with an occasional test point indicating a plasma velocity of 1800 m/sec. The total enthalpy of the plasma was 2600 Btu/lb, which should have resulted in a Mach number near 1.7 and a velocity of 1800 m/sec at the exit of the nozzle extension. Fourteen hundred m/sec is approximately sonic velocity at these conditions. As discussed in Section 2.1, for a majority of the test data the supersonic nozzle extension was not completely filled, and the Mach number at the exit was nearly sonic.

The magnetic field imposed at the electrodes appeared to have little if any effect on the plasma velocity, as can be seen in Fig. 25. Moreover, the addition of seed material to the plasma (less than 0.15 mole percent) did not seem to change the velocity measurement.

4.1.3 Image-Converter Camera with Electrode Spark Discharge and Laser Spark

The calculated centerline velocity as a function of the plasma total temperature is presented in Fig. 26. For these tests the nozzle extension was not used, and the supersonic nozzle was operating correctly. Some of the data presented are from the electrode spark and some from the laser spark. The range of velocity shown for a given total temperature is not the accuracy of the measurement but rather several test

points taken at that particular operating temperature. The arc heater did not always repeat a set operating condition. The arc heater total enthalpy was varied from 700 to 2700 Btu/lb with the resulting variation in total temperature shown in Fig. 26. Both air and nitrogen data, either seeded or unseeded, are presented in the figure. Only the laser-induced spark was visible at the 0.3-mole percent seeding rate.

The values for the theoretical line presented in Fig. 26 were derived from one-dimensional energy considerations and gas dynamic equations. As is evident from Fig. 26, the experimental points from the photographic data are, in general, higher than the theory predicts. Some explanation of this discrepancy is given in the following paragraphs.

4.2 GAS DYNAMIC VELOCITY CALCULATIONS

The theoretical values for the plasma velocity presented in Fig. 26 were calculated from one-dimensional energy considerations and gas dynamic equations. The stilling chamber total pressure, nozzle area ratio, impact pressure measurements, and an energy balance on the arc heater were used to evaluate the equations. Several uncertainties exist in these calculations and are discussed briefly.

4.2.1 Plasma Flow Field

The test media was a free jet issuing from a supersonic nozzle. A photograph of the supersonic jet discharging from the arc heater nozzle to atmosphere is shown in Fig. 27. As noted from the photograph and from the static pressure measured at the exit of the nozzle (pressure = 0.8 atm), the jet was overexpanded. The plasma total enthalpy was 2500 Btu/lb for this case.

The impact pressure in the free jet was measured axially along the plasma centerline with a pitot pressure probe. From the stilling chamber pressure and the pitot pressure measurements, the local Mach number and velocity can be calculated for an assumed ratio of specific heats if both the total pressure and the total enthalpy are assumed to remain constant along the jet centerline. These are not unreasonable assumptions since only weak oblique shock waves exist immediately downstream of the nozzle, and the heat losses in the nozzle are moderate. Using these assumptions, the velocity as a function of distance from the nozzle was calculated and is presented in Fig. 28. From this figure it can be observed that the plasma velocity is predicted to vary between 1800 and 2100 m/sec, depending on the distance downstream from the nozzle and that there are no significant regions of constant velocity.

Therefore, significant differences in the plasma velocity could be obtained depending on where the original tracer spark was placed. Arc heater fluctuations have a further detrimental effect since they would not only change the velocity of the plasma but would change the location of the shock waves and, therefore, the downstream velocity distribution. Thus, it can be seen that to predict the velocity accurately in the plasma test flow at a particular location and instant in time is an onerous task.

4.2.2 Plasma Dynamics

The plasma generated by the arc heater is not a steady flow. The unsteadiness has been observed from the variations in the plasma luminosity and shock wave locations recorded in high-speed motion-picture photographs and from measurements taken with high response instrumentation. Thus, several photographs of the tracer spark at the same plasma generator operating point could and did on many occasions yield significantly different plasma velocities.

4.2.3 Enthalpy Calculation

The enthalpy used to calculate the velocity was obtained from an energy balance on the arc heater. This calculation involves measuring the voltage and current to the arc heater, the gas water coolant flow rates, and the coolant temperature rise. The calculated enthalpy represents a time-averaged bulk enthalpy, not a local enthalpy. Since enthalpy gradients exist across the plasma, with higher enthalpies than the bulk enthalpy in the plasma core, the velocity calculated from this energy balance may be quite different than the instantaneous centerline velocity measured by the spark displacement technique.

SECTION V
CONCLUDING REMARKS

The use of a tracer spark produced by either a pair of electrodes or a focused pulse laser to determine the velocity of a high enthalpy supersonic gas (air or nitrogen) has been demonstrated. Moreover, it has been shown that the tracer spark produced by a laser could be photographed and used for a velocity determination in a seeded plasma, whereas an electrode spark arrangement was not effective. The best equipment arrangement proved to be the image-converter camera to photograph the tracer spark displacement and the focused pulse laser to produce the tracer spark. Plasma velocities up to 2600 m/sec have been measured; however, there is no reason to believe that the

equipment could not be used to measure velocities up to 8000 m/sec in any flowing gas.

REFERENCES

1. Kyser, J. B. "Development of a Tracer-Spark Technique for the Study of Hypervelocity Flow Fields." Stanford University Report SUDAER No. 190, May 1964.
2. Miller, H. R. "Shock-on-Shock Simulation and Hypervelocity Flow Measurements with Spark-Discharge Blast Waves." AIAA Paper No. 66-763, September 1966.
3. Woods, G. P., Carter, A. F., Sabol, A. P., McFarland, D. R., and Weaver, W. R. "Research on Linear Cross-Field Steady Flow D-C Plasma Accelerators at Langley Research Center, NASA." AGARDograph 84, September 1964, pp. 1-45.
4. Chen, C. J. "Velocity-Profile Measurement in Plasma Flows Using Tracers Produced by a Laser Beam." Journal of Applied Physics, Vol. 37, No. 8, July 1966, pp. 3092-3095.
5. "Noninterference Instrumentation for Scramjet Combustors." The Marquardt Corporation, Report No. 25, November 1967, p. 239.
6. Minck, R. W. "Optical Frequency Electrical Discharges in Gases." Journal of Applied Physics, Vol. 35, 1964, pp. 252-254.
7. Meyerand, R. G., Jr. "Laser Plasma Production - A New Area of Plasmadynamics Research." AIAA Journal, Vol. 5, No. 10, 1967, pp. 1730-1737.
8. Frederick, O. M., Jr. and Weigl, F. "Investigation of Strong Blast Waves and Dynamics of Laser Induced Plasma in High Pressure Gases." AIAA Electric Propulsion and Plasmadynamics Conference, AIAA Paper No. 67-696, September 11-13, 1967.

APPENDIX
ILLUSTRATIONS

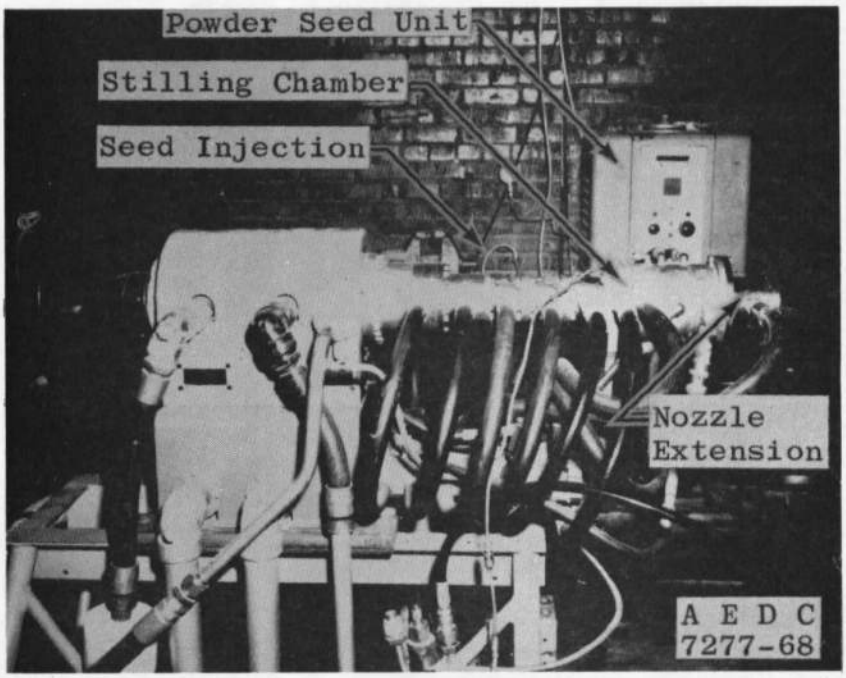

Fig. 1 Photograph of the Electric Arc Heater Installation

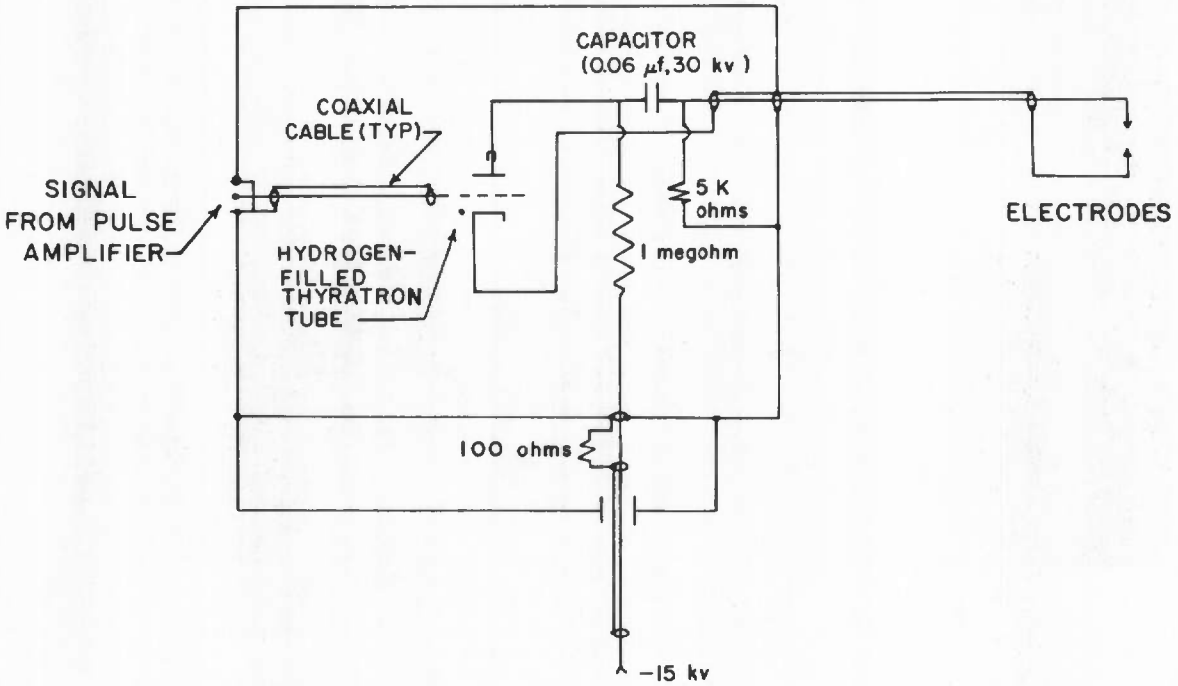

Fig. 2 Schematic of the 15-kv Electrode Power Supply

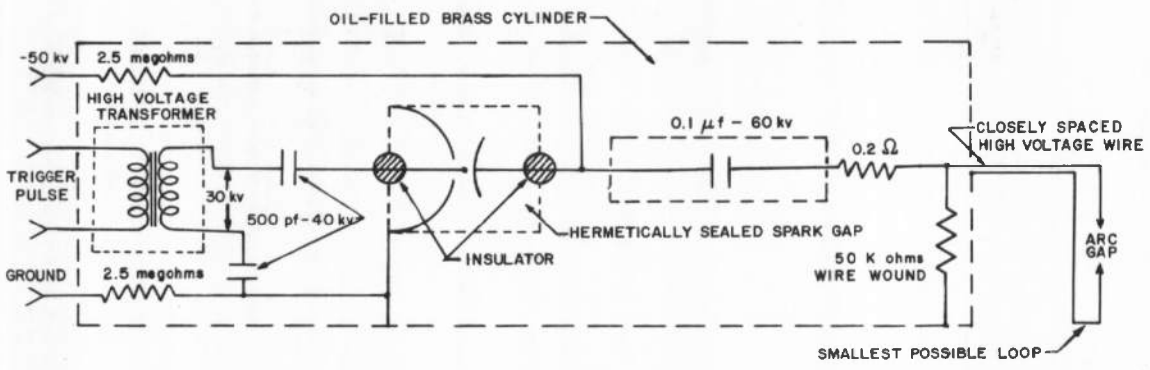

Fig. 3 Schematic of the 50-kv Electrode Power Supply

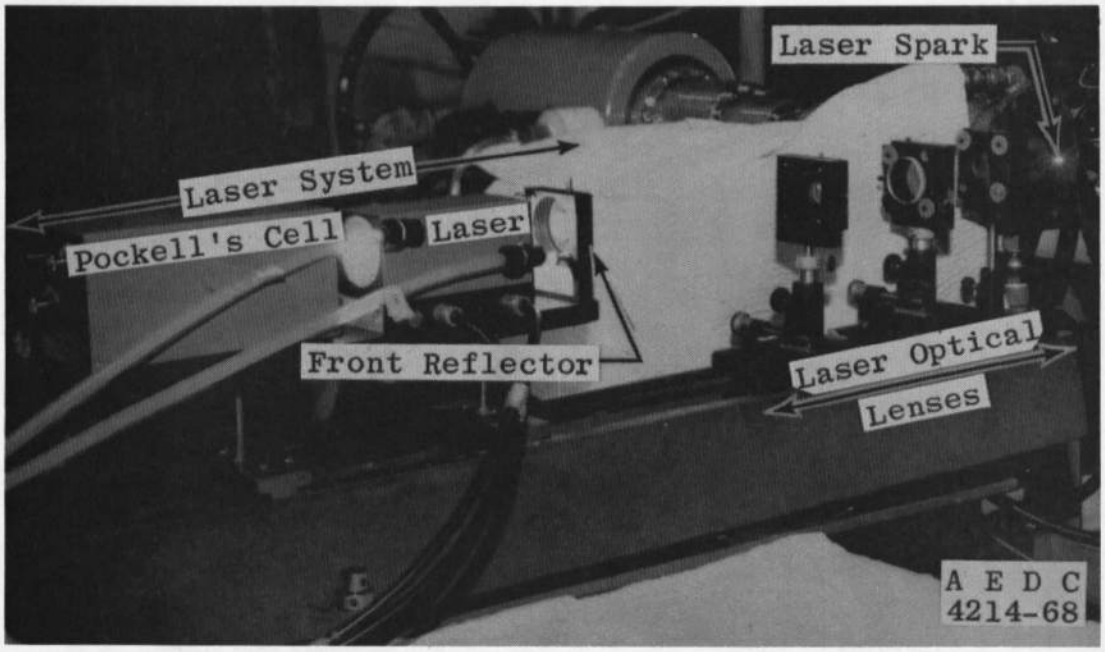

Fig. 4 Photograph of the Laser Installation

LENS	TYPE LENS	FOCAL LENGTH (f_L), mm	LENS DIA mm
L_1	Plano-Concave	−50	20
L_2	Acromatic	180	58
L_3	Plano-Convex	120	58

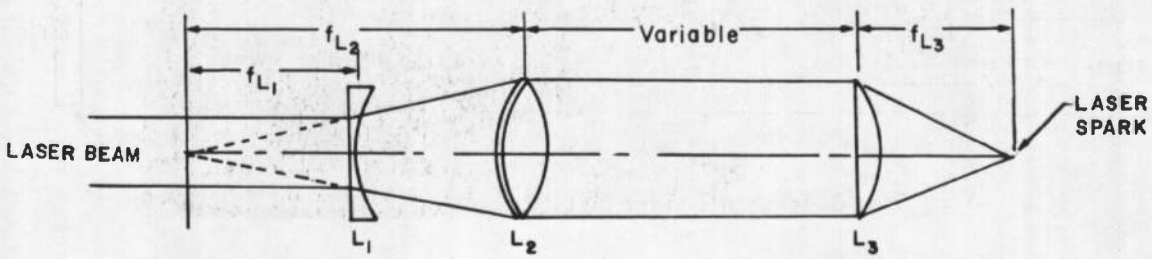

Fig. 5 Schematic of the Laser Optics

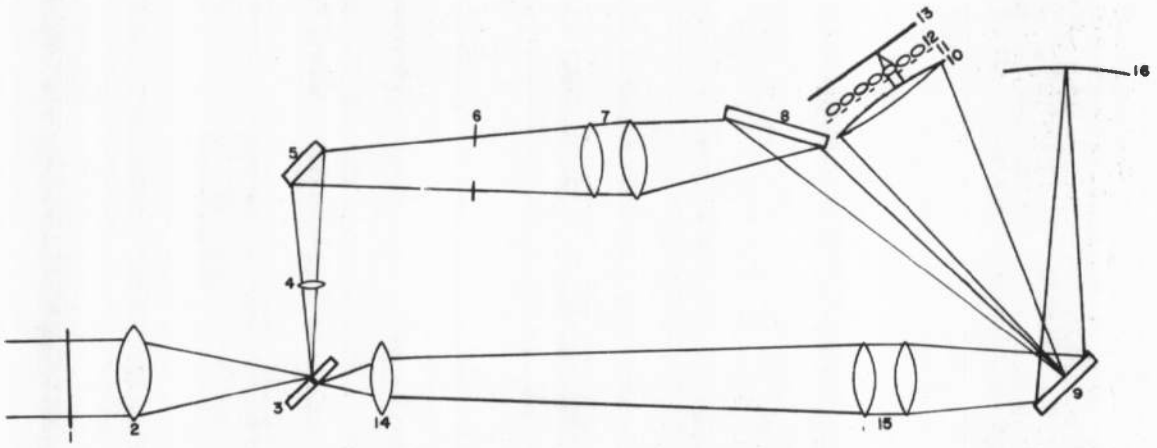

1. CAPPING SHUTTER
2. OBJECTIVE LENS
3. SLIT AND RELAY MIRROR
4. FIELD LENS
5. FRONT RELAY MIRROR
6. PRIMARY FRAMING STOP
7. FRAMING RELAY LENSES
8. REAR RELAY MIRROR
9. ROTATING MIRROR
10. PROJECTION LENS
11. SECONDARY STOPS
12. IMAGING LENSES
13. FRAMING CAMERA FILM PLANE
14. FIELD LENS
15. STREAK CAMERA RELAY LENSES
16. STREAK CAMERA FILM PLANE

Fig. 6 Schematic of the Streak and Framing Camera

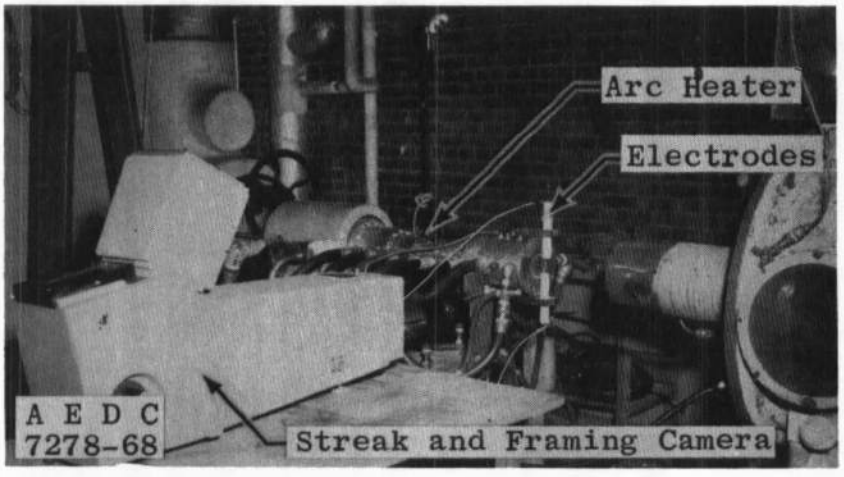

Fig. 7 Photograph of the Installation of the Streak and Framing Camera

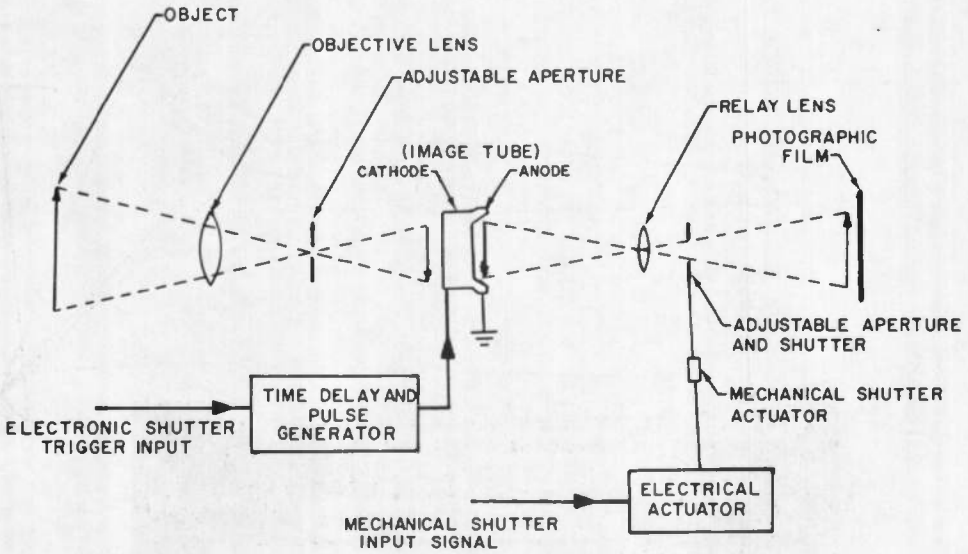

Fig. 8 Schematic of the Image-Converter Camera

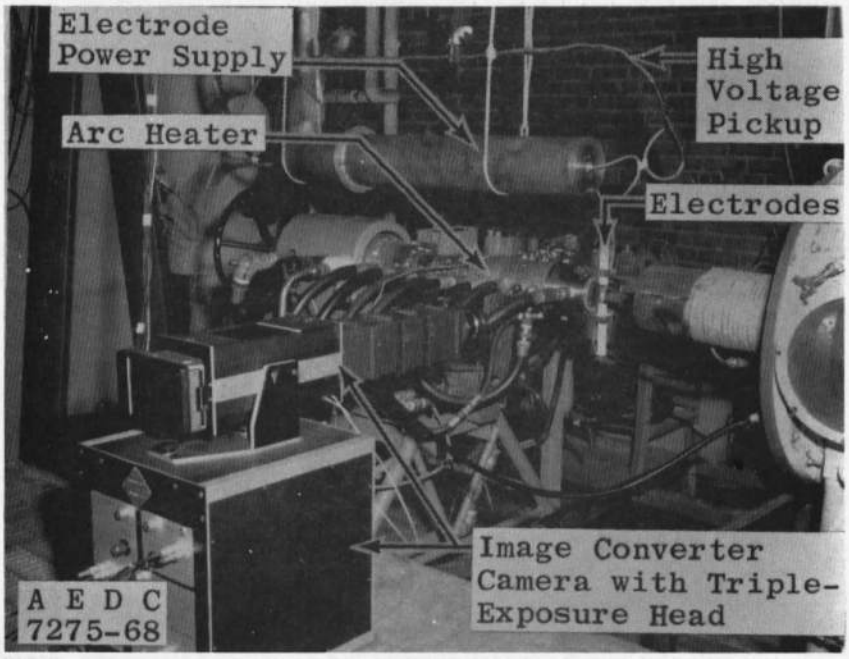

Fig. 9 Photograph of the Installation of the Image-Converter Camera

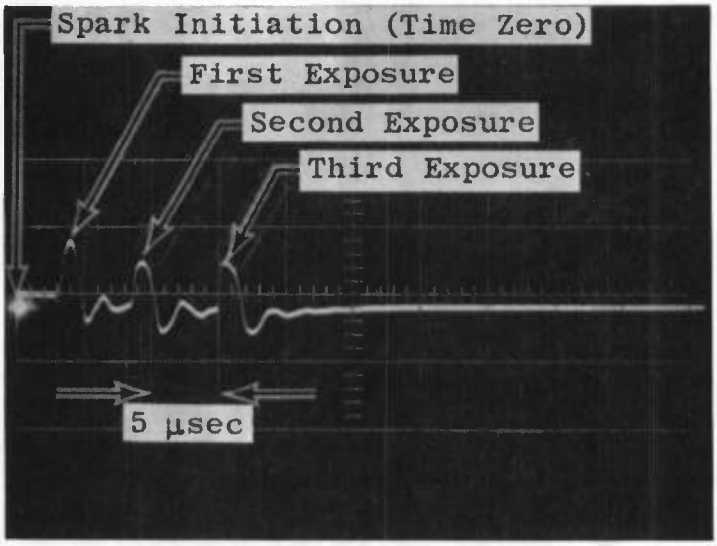

Fig. 10 Typical Oscilloscope Time Record

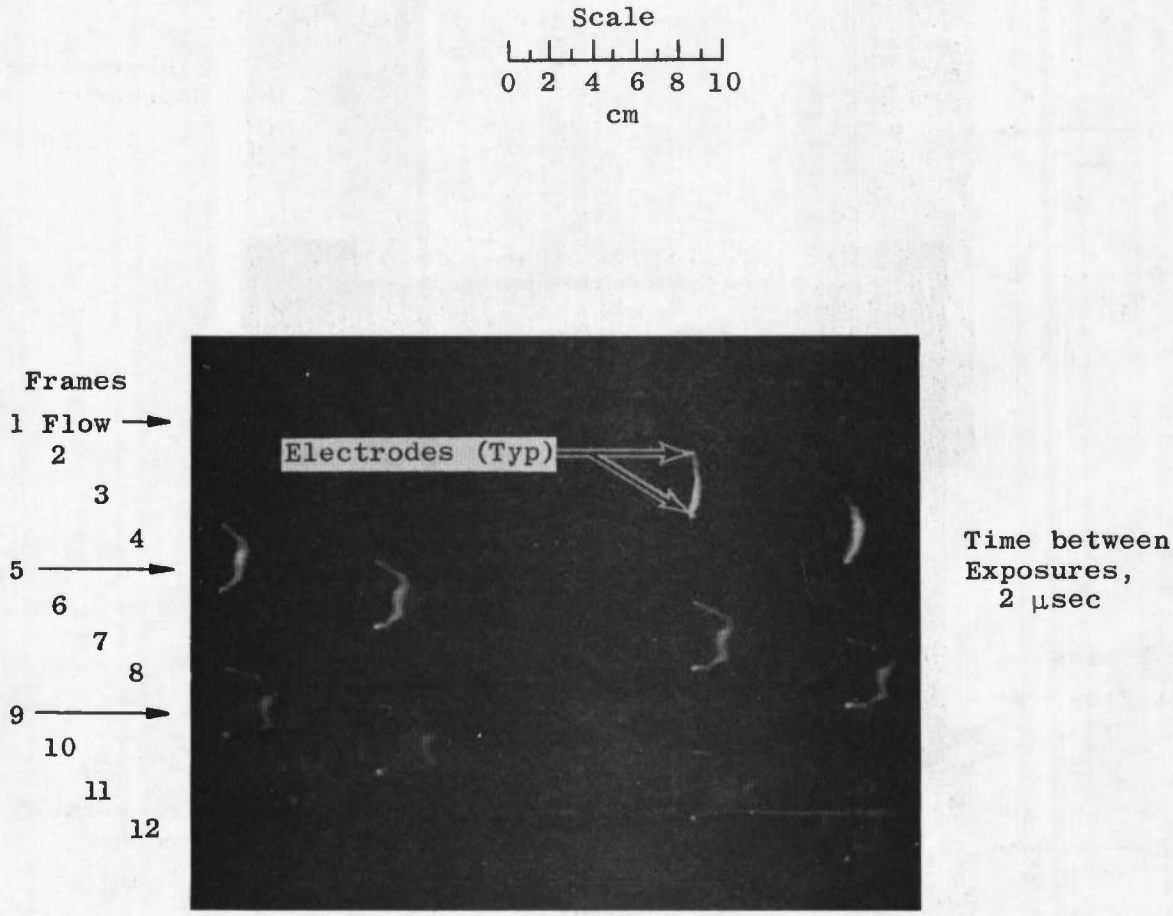

a. Electrode Spark in Unseeded Plasma

Fig. 11 Streak and Framing Camera Photographs

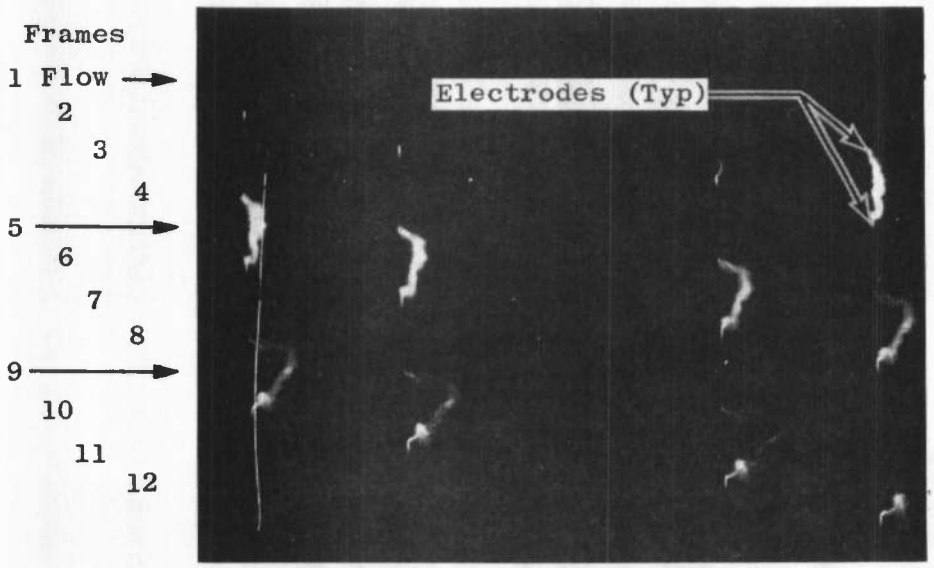

b. Electrode Spark in Unseeded Plasma with Electrode Protruding into Plasma

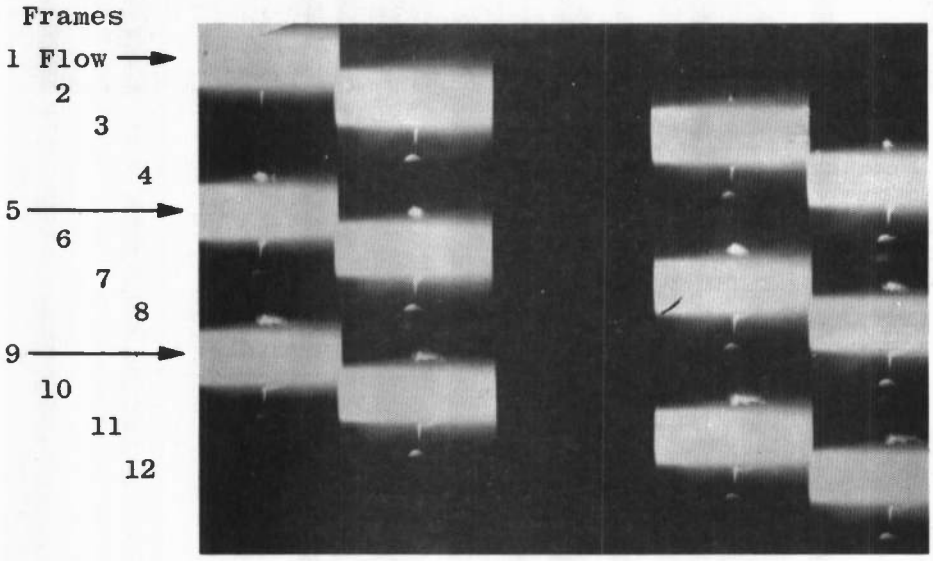

c. Electrode Spark in Seeded Plasma

Fig. 11 Concluded

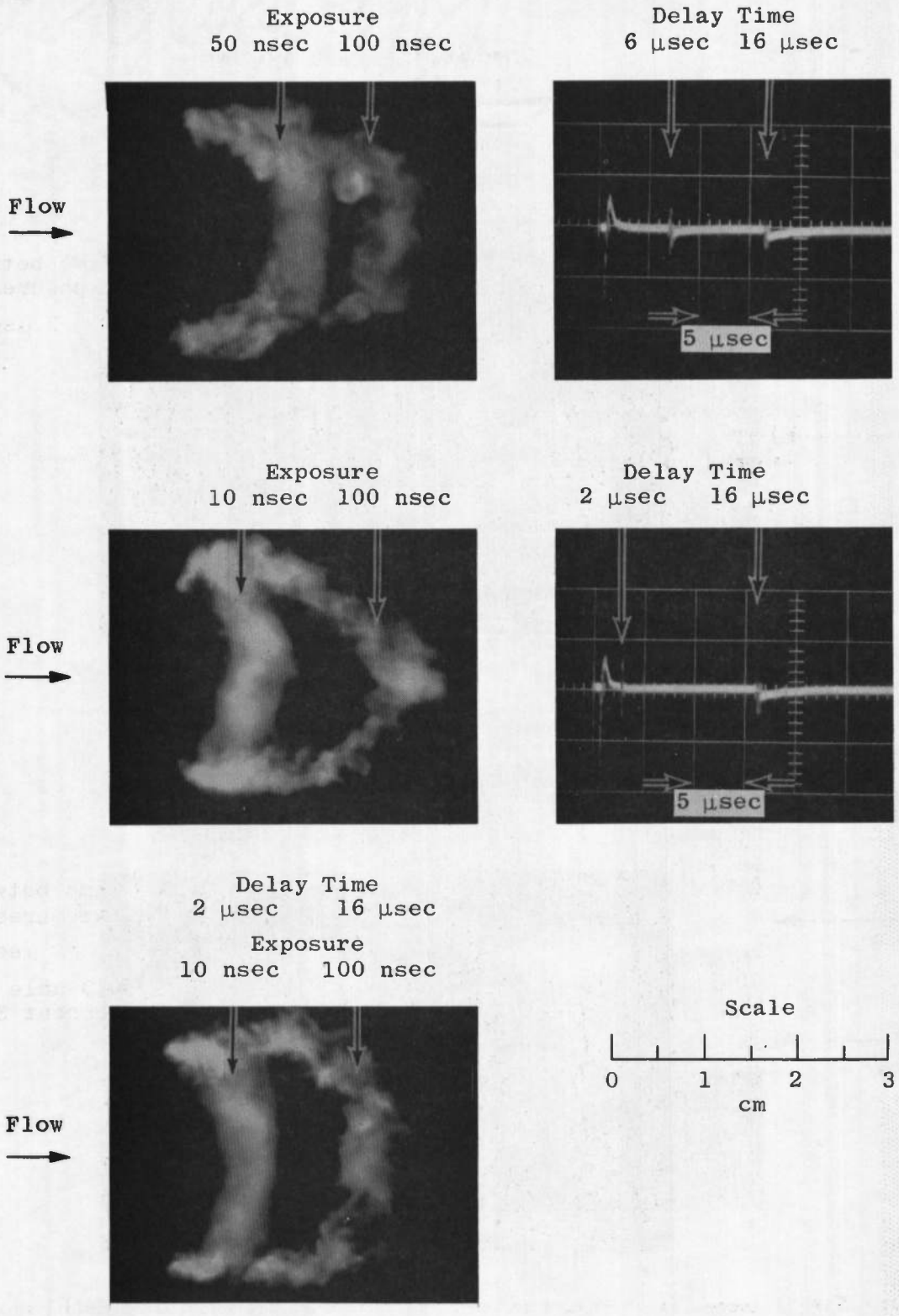

Fig. 12 Image-Converter Camera Photographs with Electrode Spark and Nozzle Extension (Unseeded Plasma)

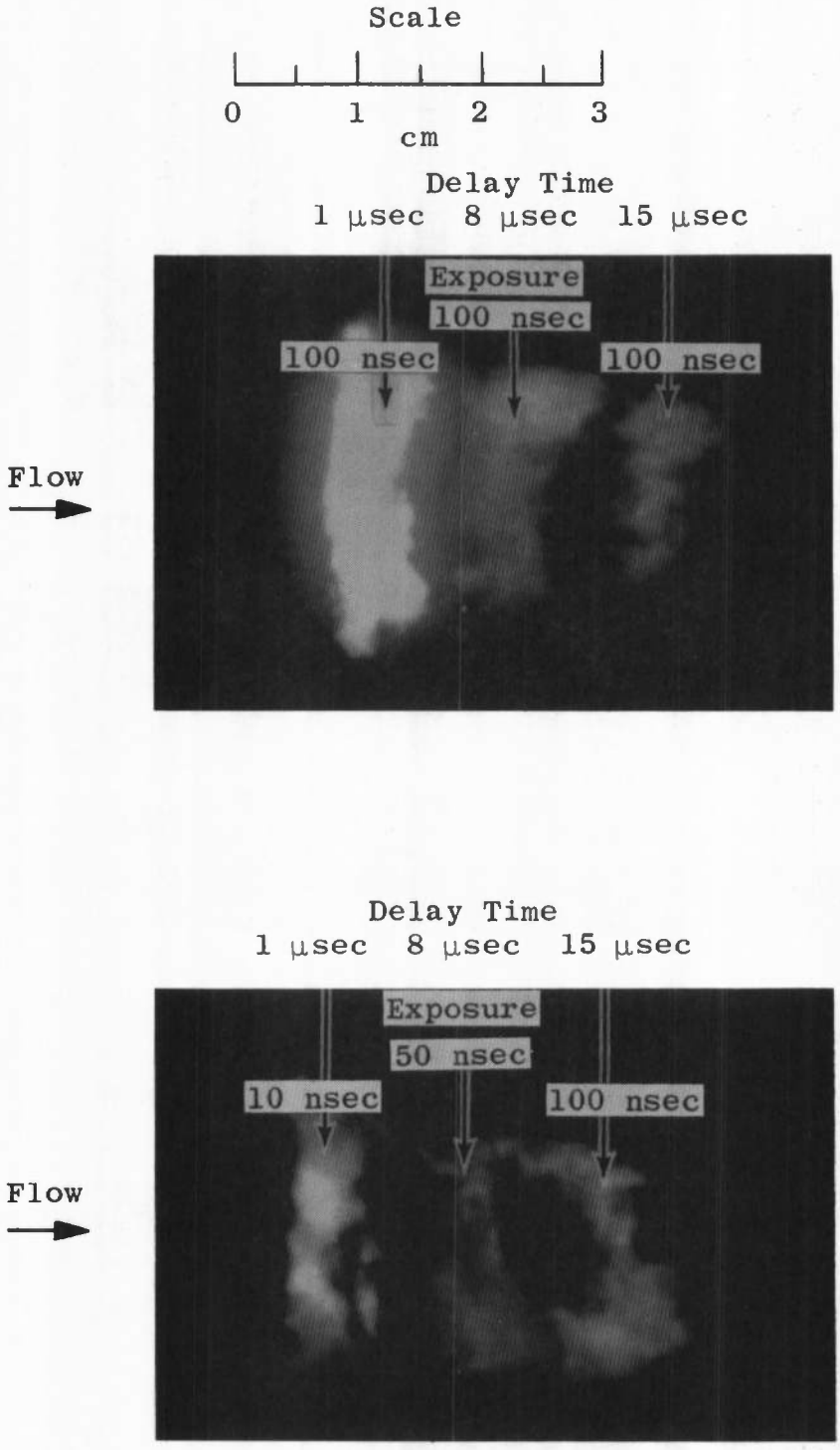

Fig. 13 Image-Converter Camera Photographs with Electrode Spark (Unseeded Plasma)

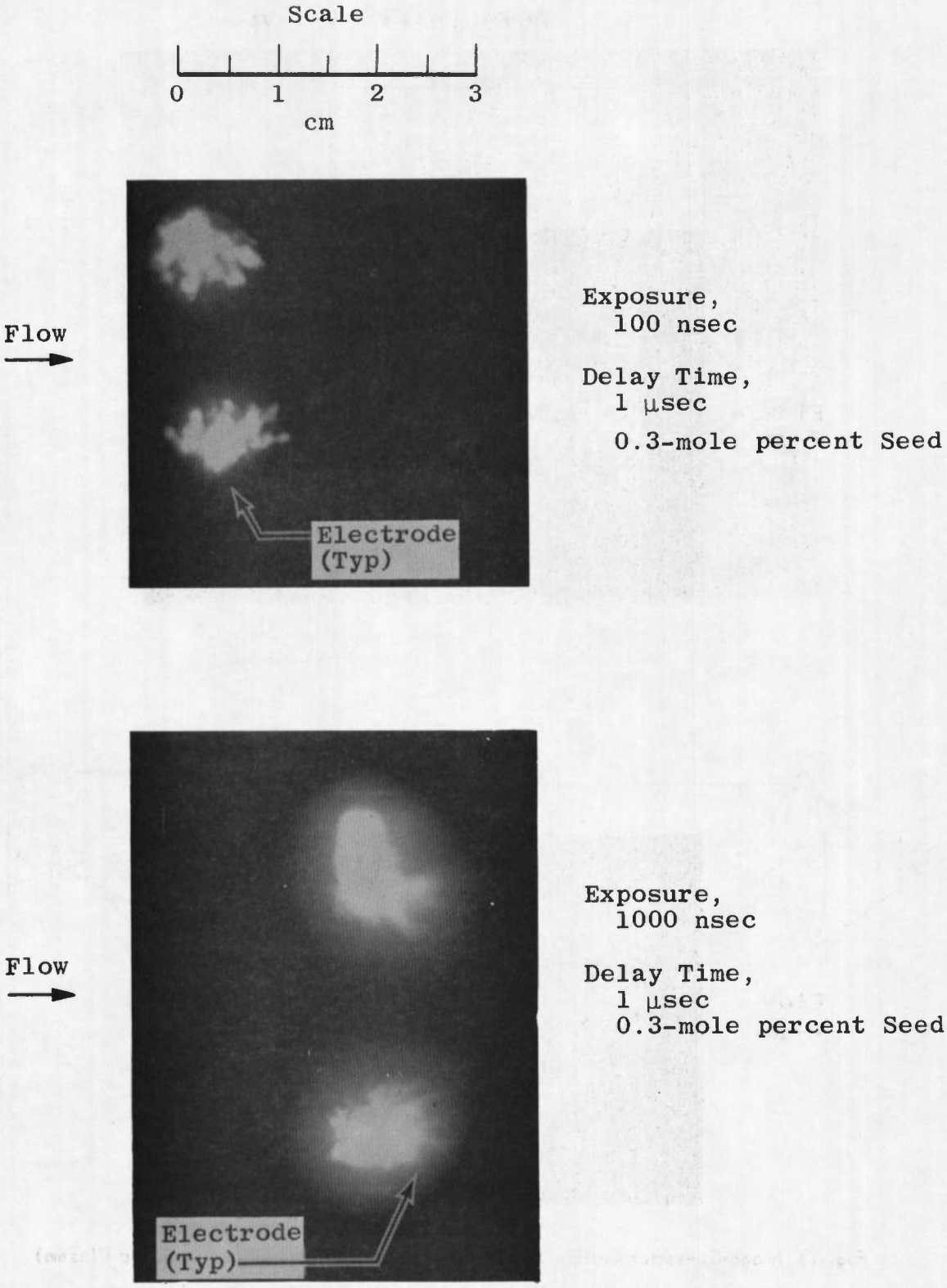

Fig. 14 Image-Converter Camera Photographs with Electrode Spark (Seeded Plasma)

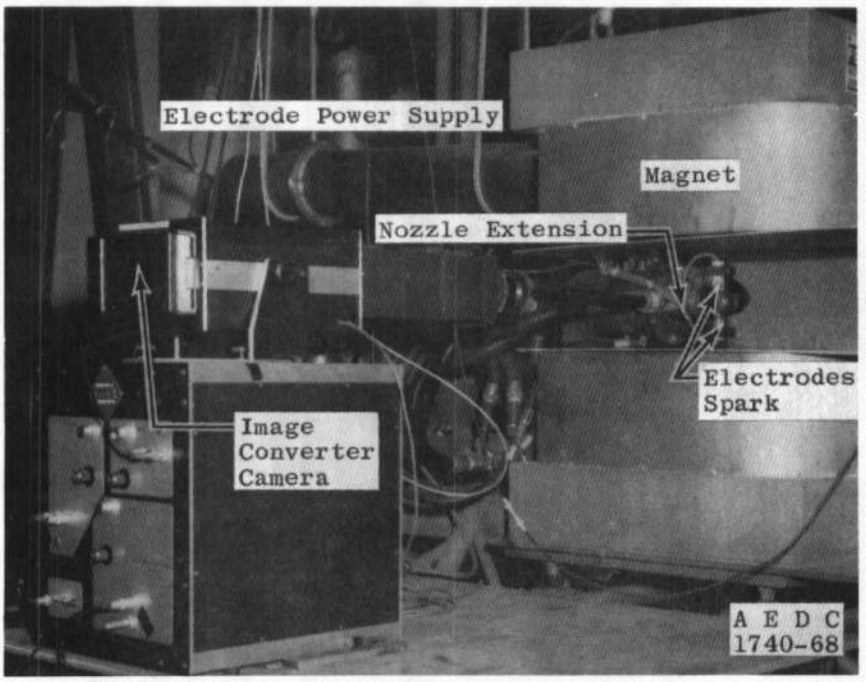

Fig. 15 Photograph of the Magnetic Installation Used with the Image-Converter Camera and Electrode Spark

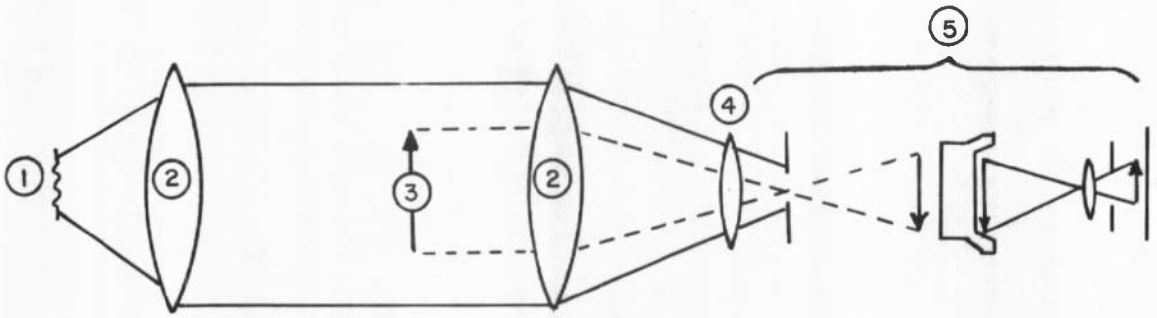

1. SPARK LIGHT SOURCE
2. BICONVEX LENS
3. OBJECT
4. CAMERA OBJECTIVE LENS
5. IMAGE CONVERTER CAMERA

Fig. 16 Schematic of the Shadowgraph System Used with the Image-Converter Camera and Electrode Spark

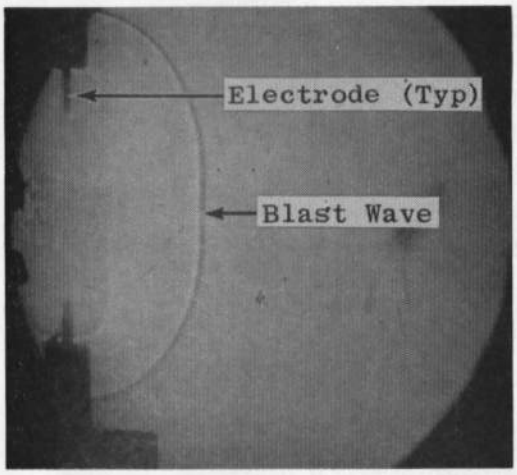

Scale

0 1 2 3 4

cm

25-μsec Delay
1-nsec Exposure

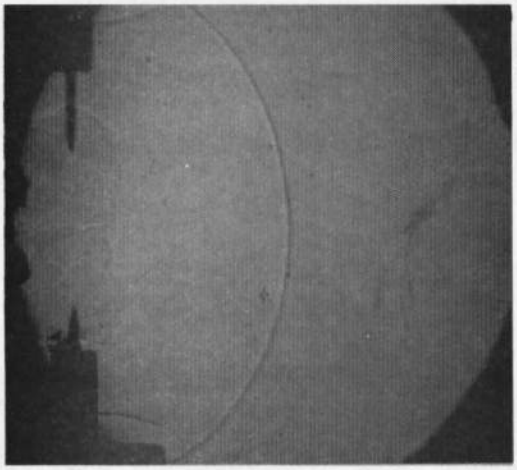

55-μsec Delay
1-nsec Exposure

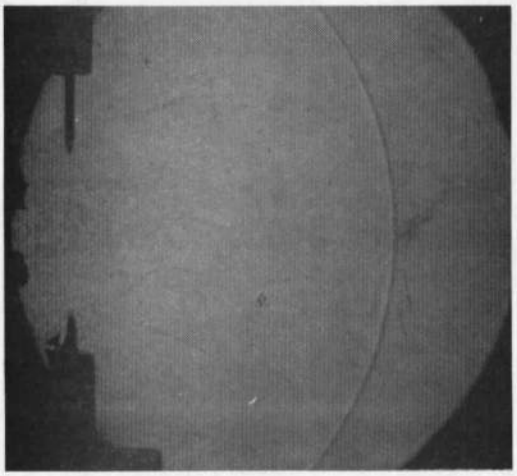

88-μsec Delay
1-nsec Exposure

Fig. 17 Photograph of the Blast Wave Obtained with the Image-Converter Camera and Electrode Spark in Quiescent Air

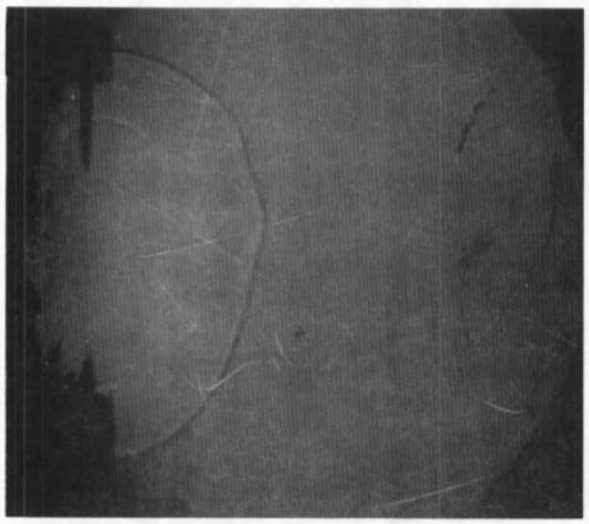

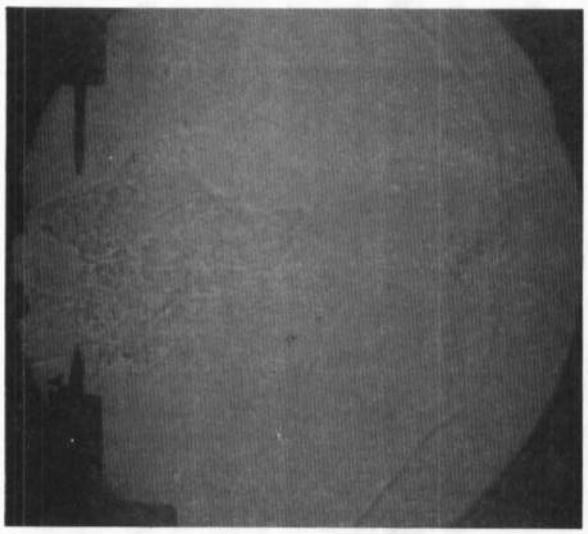

Fig. 18 Photograph of the Blast Wave Obtained with the Image-Converter Camera and Electrode Spark in Low Velocity Nitrogen

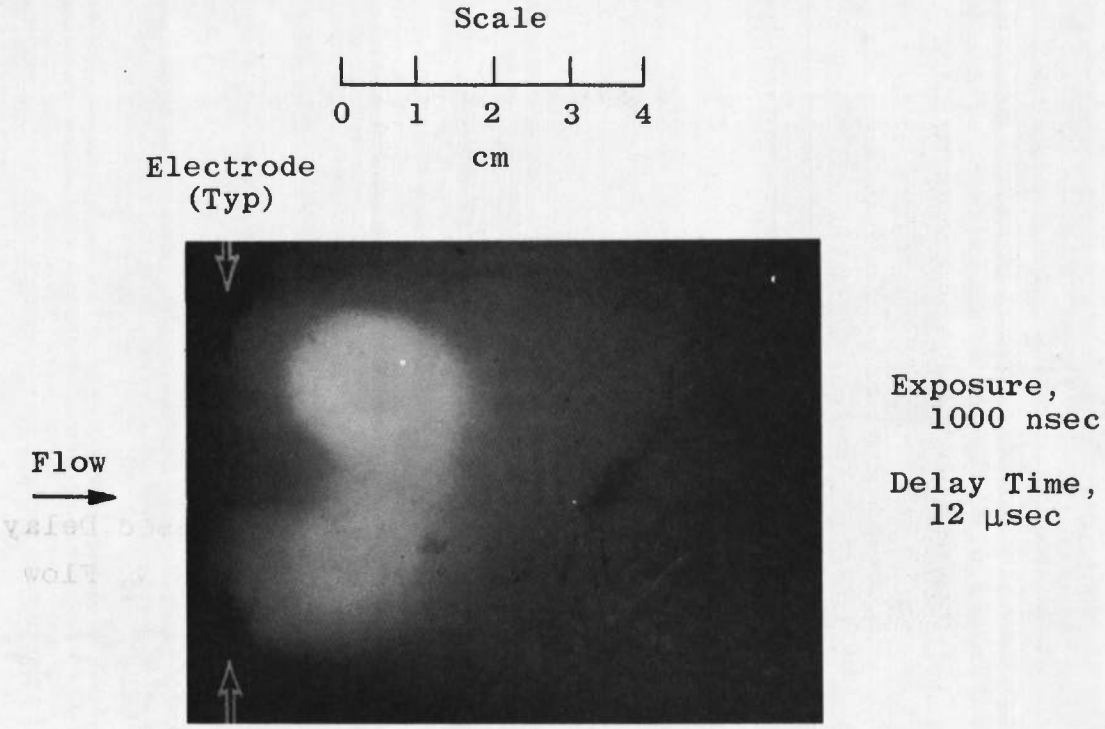

Fig. 19 Photographs with the Shadowgraph System in the High Enthalpy Plasma (Unseeded)

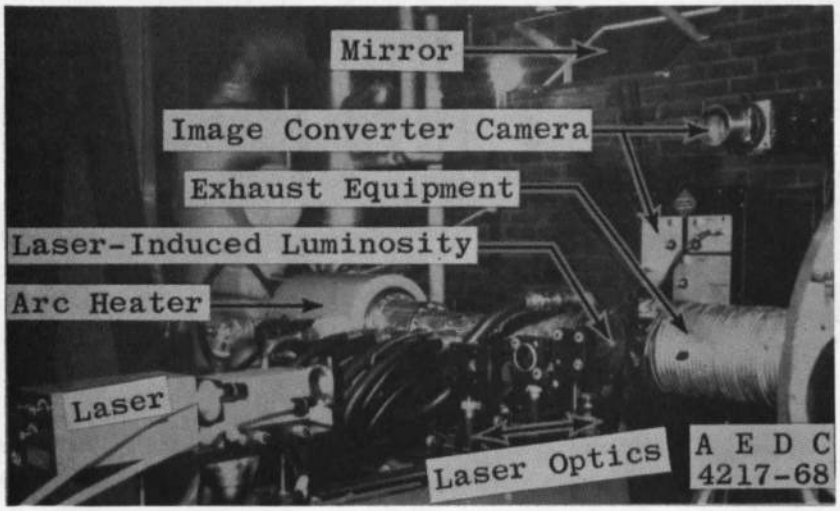

Fig. 20 Photograph of the Laser Test Installation

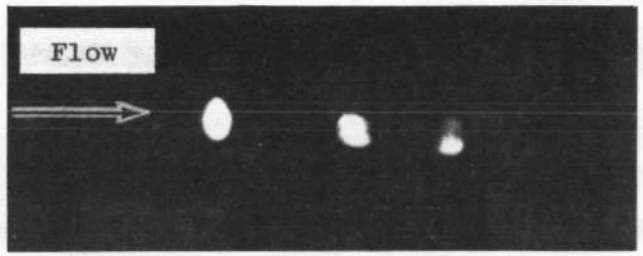

Scale 0 1 2 3 cm

Delay Time, 1.0, 7.5, and 12.8 μsec
Exposure Time, 0.1, 1.0, and 1.0 μsec
Total Enthalpy = 2500 Btu/lb
Seed, None

a. Unseeded Nitrogen Plasma

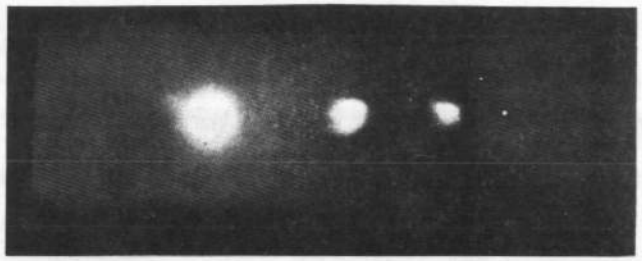

Delay Time, 1.0, 7.5, and 13.0 μsec
Exposure Time, 0.1, 1.0, and 1.0 μsec
Total Enthalpy = 2350 Btu/lb
Seed, 0.3-mole percent

b. Seeded Nitrogen Plasma

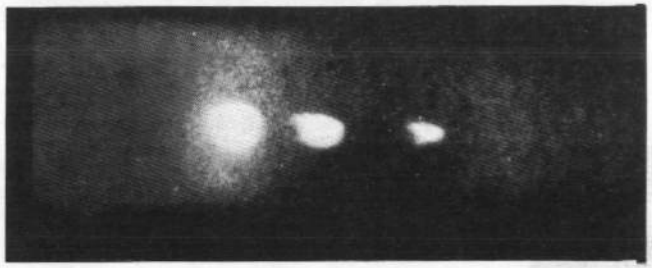

Delay Time, 3.0, 8.8, and 15.0 μsec
Exposure Time, 1.0, 1.0, and 1.0 μsec
Total Enthalpy = 2550 Btu/lb
Seed, 0.3-mole percent

c. Seeded Air Plasma

Fig. 21 Laser Spark Photographs

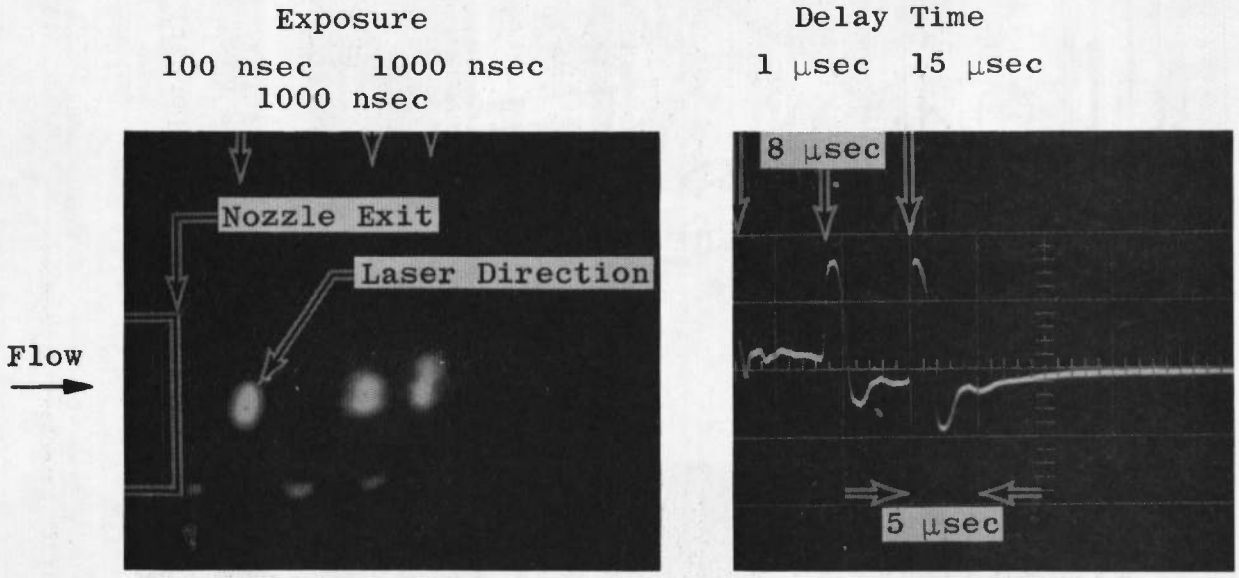

Fig. 22 Photograph of a Multiple Laser Spark in a Seeded Nitrogen Plasma

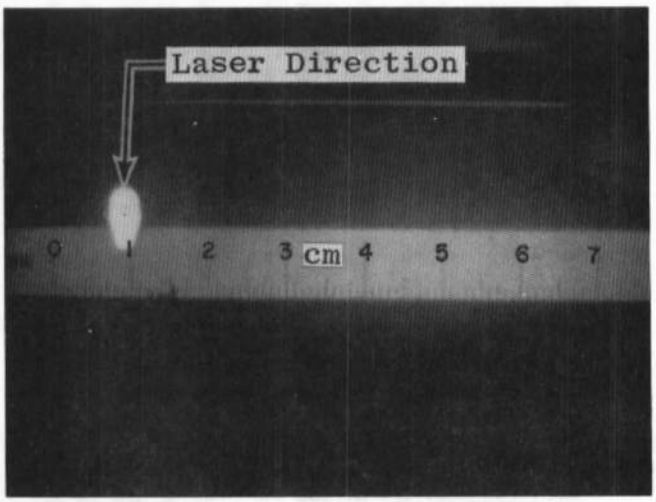

a. High Laser Power

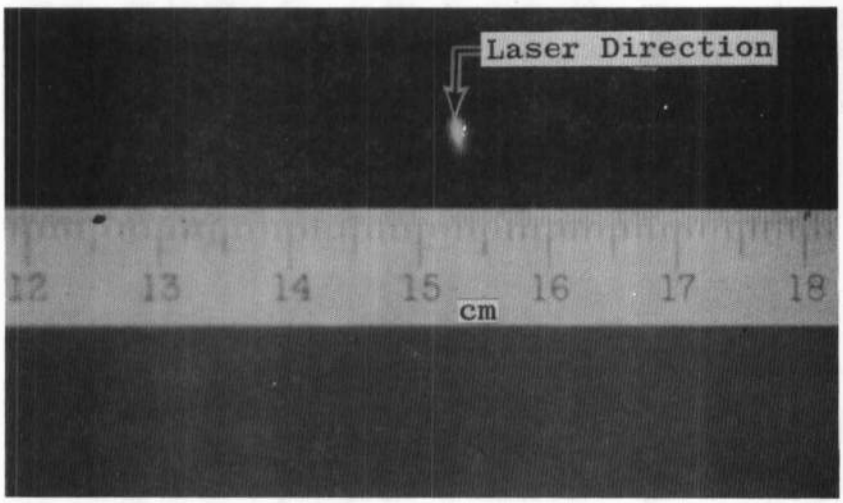

b. Low Laser Power

Fig. 23 Photograph of the Laser Spark in Quiescent Air

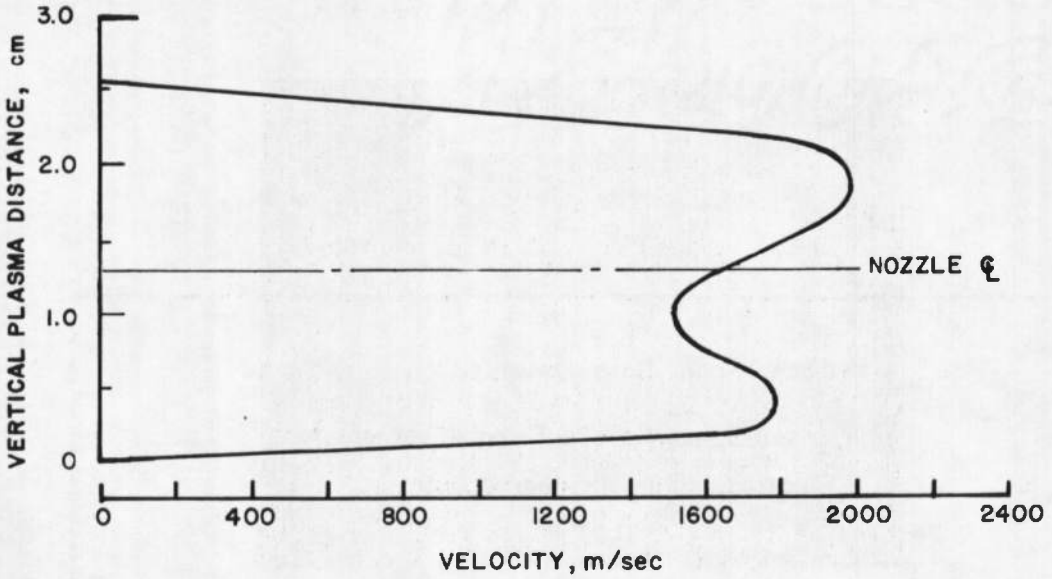

Fig. 24 Plasma Velocity Profile Obtained with the Streak and Framing Camera (Unseeded Plasma)

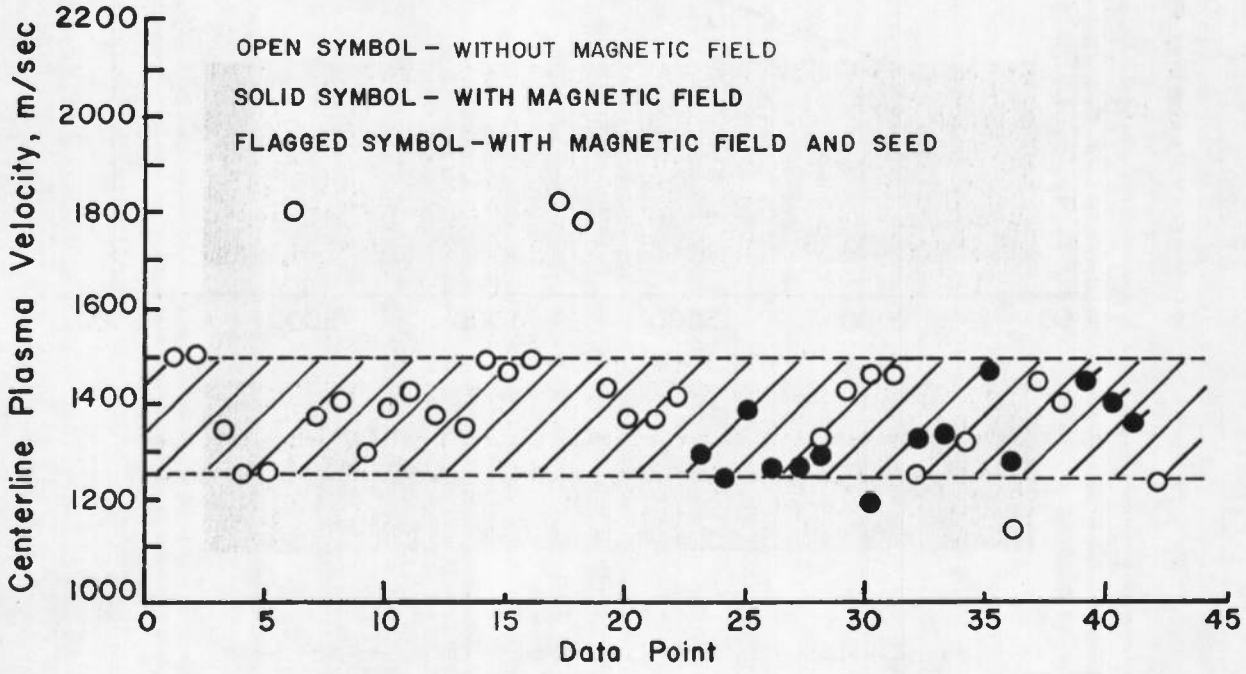

Fig. 25 Compilation of Centerline Velocity Data Obtained with the Image-Canverter Camera and Electrode Spark

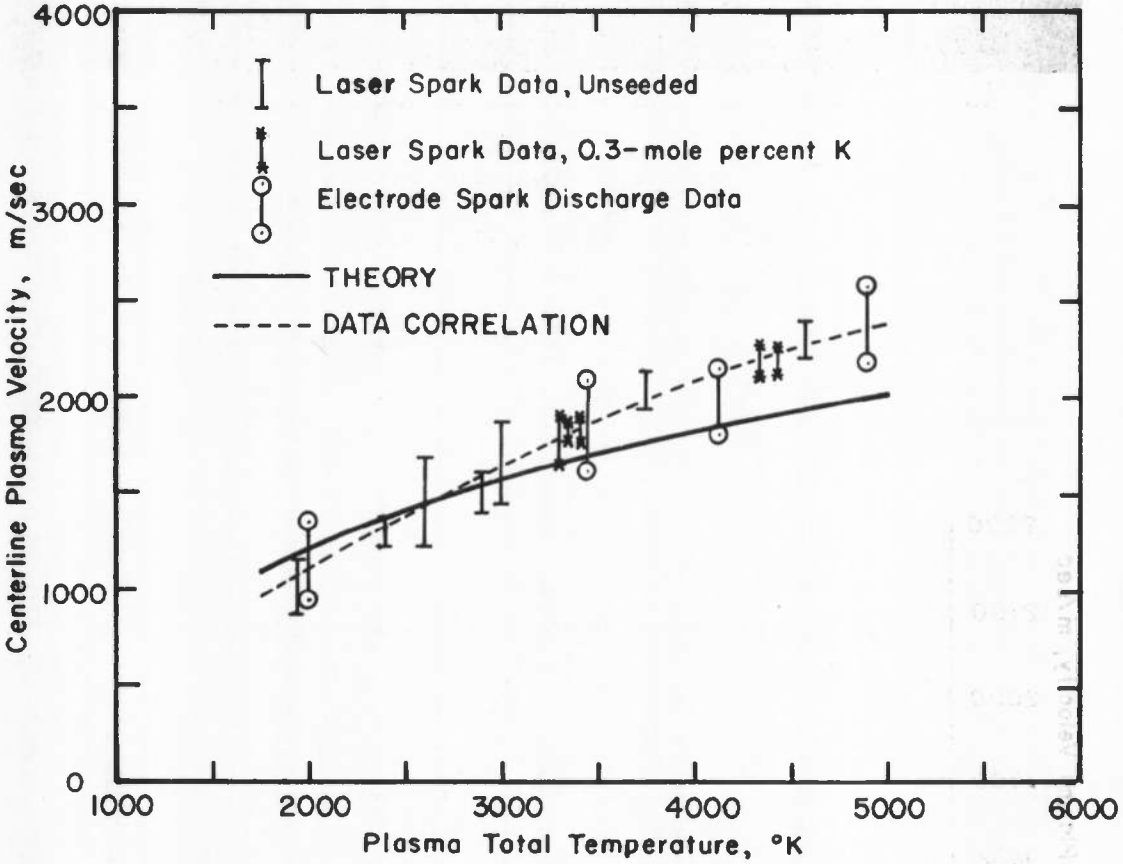

Fig. 26 Velocity Measurements as a Function of Plasma Tatal Temperature Obtained with the Image-Converter Camera and the Electrode Spark and Laser Spark

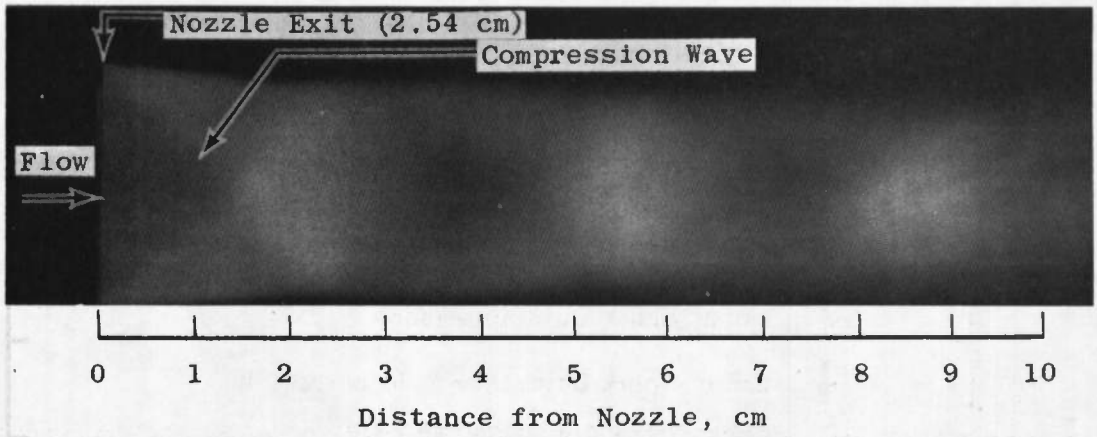

Fig. 27 Photograph of the Plasma Exhaust Jet

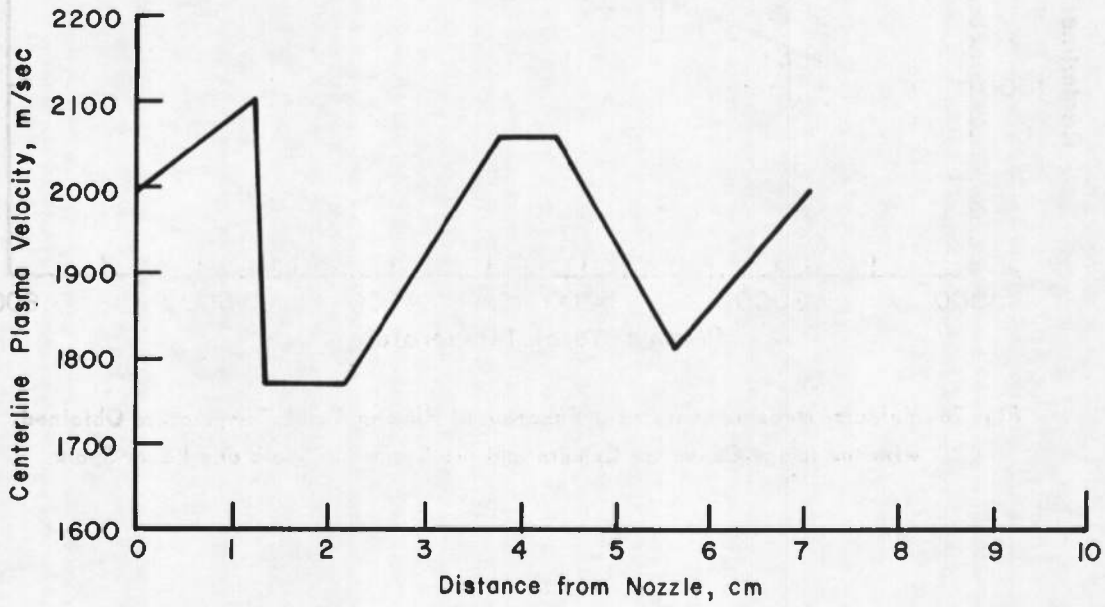

Fig. 28 Calculated Plasma Velocity as a Function of Distance Downstream of the Nozzle

UNCLASSIFIED
Security Classification

DOCUMENT CONTROL DATA - R & D

(Security classification of title, body of abstract and indexing annotation must be entered when the overall report is classified)

1. ORIGINATING ACTIVITY *(Corporate author)*
Arnold Engineering Development Center
ARO, Inc., Operating Contractor
Arnold Air Force Station, Tennessee

2a. REPORT SECURITY CLASSIFICATION
UNCLASSIFIED

2b. GROUP
N/A

3. REPORT TITLE
NONINTERFERENCE VELOCITY MEASUREMENTS IN A SUPERSONIC SEEDED PLASMA USING TRACERS PRODUCED BY A SPARK DISCHARGE AND A FOCUSED PULSED LASER

4. DESCRIPTIVE NOTES *(Type of report and inclusive dates)*
November 1966 to July 1968 - Final Report

5. AUTHOR(S) *(First name, middle initial, last name)*
J. C. Pigott and L. E. Rittenhouse, ARO, Inc.

6. REPORT DATE
November 1968

7a. TOTAL NO. OF PAGES
46

7b. NO. OF REFS
8

8a. CONTRACT OR GRANT NO. F40600-69-C-0001

b. PROJECT NO. 4344

c. Program Element 6540215F

d Task 434409

9a. ORIGINATOR'S REPORT NUMBER(S)
AEDC-TR-68-235

9b. OTHER REPORT NO(S) *(Any other numbers that may be assigned this report)*
N/A

10. DISTRIBUTION STATEMENT
This document has been approved for public release and sale; its distribution is unlimited.

11. SUPPLEMENTARY NOTES
Available in DDC.

12. SPONSORING MILITARY ACTIVITY
Arnold Engineering Development Center, Air Force Systems Command, Arnold Air Force Station, Tennessee 37389

13. ABSTRACT

Experimental results are presented from a program conducted to develop a noninterference method for obtaining the velocity of a supersonic, high enthalpy plasma seeded with an alkali metal. The technique used was the time-of-flight measurement of a tracer spark produced in the plasma by an electric spark discharge (two pointed electrodes) and by a focused pulse laser. The tracer spark was photographed with a streak and framing camera or an image-converter camera at preselected delay times to obtain the time-of-flight velocity measurements. The experimental work was accomplished in air and nitrogen plasmas, at a static pressure of about 1 atm and at total enthalpies up to 2700 Btu/lb. Velocities were measured up to 2600 m/sec. The techniques used are described, and the problems and results are discussed.

DD FORM 1 NOV 65 1473

UNCLASSIFIED
Security Classification

14 KEY WORDS	LINK A		LINK B		LINK C	
	ROLE	WT	ROLE	WT	ROLE	WT
seeded plasmas						
alkali metals						
electric sparks						
ruby lasers						
velocity measurement						
supersonic flow						
high speed photography						

AFSC
Arnold AFS Tenn